Table 3. Microarray Analysis

	CCl_4 + BMC vs. CCl_4 Alone	
	Increased	Decreased
MMP-2	1.7	
MMP-9	3.9	
MMP-14	2.1	
TIMP-3		0.67

NOTE. Mice were treated with CCl_4 for 4 weeks and were killed 1 week after BMC transplantation. Microarray analysis was performed using 3 livers from each group. The expression ratios (CCl_4 + BMC vs. CCl_4 alone) larger than 1.5 are shown. Values indicated are the difference between the mean values of 3 mice. Results are typical of 1 of 2 independent experiments.

coinciding with the location of MMP-9–positive BMCs compared with the liver treated with CCl_4 alone (Fig. 8).

This gelatinolytic activity was completely blocked by the addition of 1,10-phenanthroline, an MMP inhibitor (data not shown).

Finally, the mice that underwent BMC transplantation with continuous CCl_4 injection showed a gradually increased serum albumin level (Supplementary Fig. 3) resulting in a significantly improved survival rate after BMC transplantation compared with mice treated with CCl_4 alone (Supplementary Fig. 4).

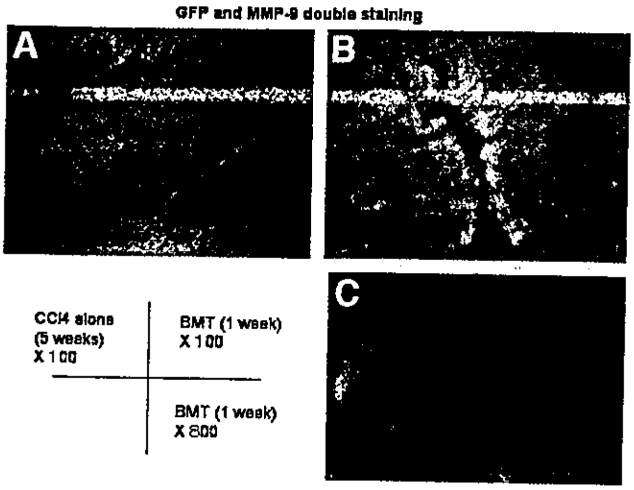

Fig. 6. Double fluorescent immunohistochemistry of a mouse liver after (A) 5-week treatment with CCl_4 alone and (B, C) 1 week after BMC transplantation (BMT) with CCl_4 treatment for 5 weeks. (Original magnification, [A and B] ×100; [C] ×800.)

Discussion

In this report, transplanted BMCs can degrade collagen fibers and clearly reduce liver fibrosis with strong expression of MMPs, especially MMP-9, as indicated by both *in situ* zymography and the double staining of GFP and MMP-9 using fluorescent microscopy. The reason for the strong expression of MMP-9 is still unknown. However, Heissing et al.[20,21] recently reported that MMP-9 induced in BMCs released soluble Kit-ligand, which might be related to the transfer of stem cells in BMCs to the proliferative niche. Therefore, MMP-9 in our model could play an important role in the degradation of extracellular matrix and also by releasing some factors, *e.g.*, soluble Kit-ligand, related to the differentiation and proliferation of transplanted BMCs in liver inflammation induced by continuous injection of CCl_4. It has also been shown that MMP-9 plays an important role in the migration of mast progenitor cells to inflammatory

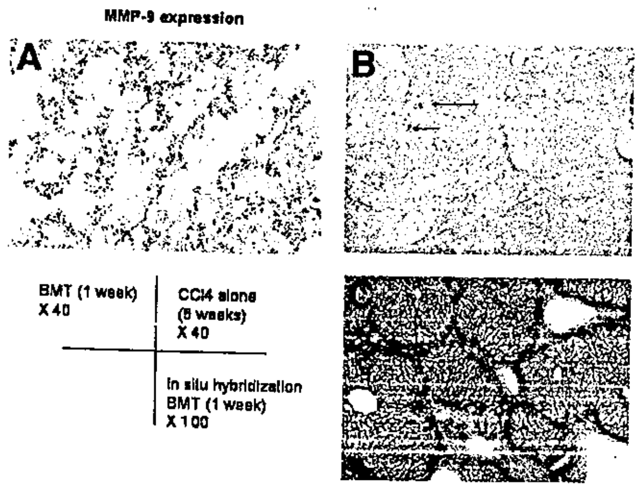

Fig. 5. Photomicrograph of a liver section stained with anti-MMP-9 antibody (A) from a mouse 1 week after BMC transplantation (BMT) and (B) from a mouse treated with CCl_4 alone for 5 weeks. (Original magnification, ×40.) (C) *In situ* hybridization of a liver section from a mouse 1 week after BMC transplantation. (Original magnification, ×100.)

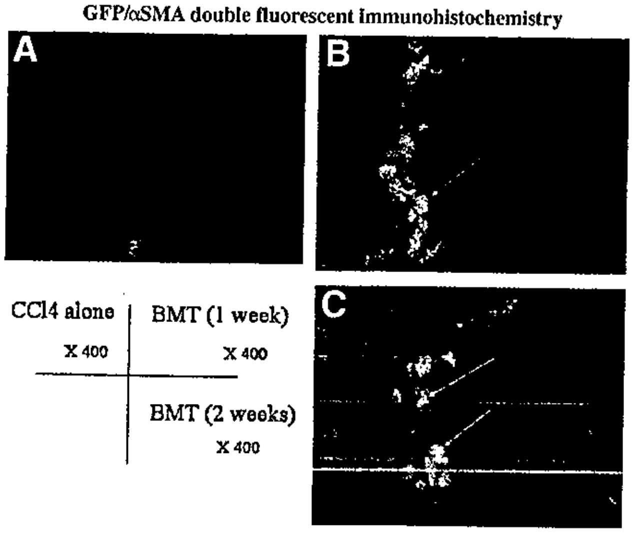

Fig. 7. Double fluorescent immunohistochemistry for α-smooth muscle actin (αSMA) and GFP of a mouse liver (A) treated with CCl_4 alone for 5 weeks and (B) 1 week, or (C) 2 weeks after BMC transplantation (BMT) with CCl_4 treatment. (Original magnification, ×400.)

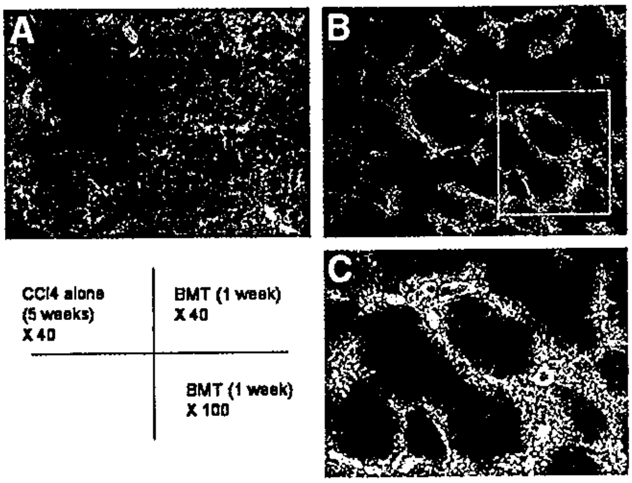

Fig. 8. *In situ* zymography of a mouse liver after (A) 5-week treatment with CCl_4 alone and (B, C) 1 week after BMC transplantation (BMT) with CCl_4 treatment for 5 weeks. (Original magnification, [A] ×40; [B] ×40, [C] ×100.)

tissue.[22,23] Therefore, the increased expression of MMP-9 in this study was somehow related to the migration of BMCs to the inflammatory liver.

Film *in situ* zymography clearly showed that these MMP-9–positive cells possessed high gelatinolytic activity compared with the liver treated with CCl_4 alone. Thus, the BMCs that migrated acted in the degradation of liver fibrosis (fibrolysis).

According to our present data, increased expression of MMP-14 (MT1-MMP [membrane-type 1 matrix metalloproteinase]) will contribute to degrading interstitial collagens[24] to gelatin that MMP-9 can degrade, resulting in the regression of fibrosis (fibrolysis).

Recently, Kollet et al.[25] reported that the expression of MMP-9 was increased with the migration of human $CD34^+$ progenitor cells in CCl_4-treated NOD/SCID mice and that an inhibitor of MMP-9 reduced this migration. Thus, proteolytic activity seems to be necessary for the cell migration in addition to matrix degradation activity.

It seems to be very important how many cells can migrate into the damaged liver to degrade fibers, but a recent paper[26] reported little evidence of bone marrow-derived hepatocytes in the CCl_4-treated liver. However, the dose of CCl_4 was only 4% (0.08 mL/kg) of our dose (0.5 mL/kg), and the number of mice used was too small (1 or 2). The reason they did not see the BMCs that migrated is most likely due to the cessation of CCl_4 injection after BMC transplantation. Even in our experimental model,[11] the cessation of CCl_4 after BMC transplantation dramatically reduced the number of BMCs migrating into the damaged liver (I.S., unpublished data, 2003). Thus, the extent of continuing liver damage may limit BMC migration to the liver with matrix degradation activity.

Transplanted BMCs differentiated into albumin-producing hepatocytes with an increased serum albumin level, and the degradation of the extracellular matrix may presumably lead to improved liver function resulting in better survival of mice with BMCtransplantation compared to that of treated with CCl_4 alone, although only 1 transplantation of BMCs was performed.

As shown by double fluorescence, our data may also indicate that transplanted BMCs seem to become stellate cells, in agreement with a recent report,[27] although the number was very small in our experimental model. This result seems to be contradictory to our result of resolution of liver fibrosis by BMC transplantation because transdifferentiated stellate cells may produce collagens. Our preliminary results indicated reduced messenger RNA expression of type I procollagen, transforming growth factor-β1 (TGF-β1) and no change of hepatocyte growth factor messenger RNA expression in the liver 1 week after BMC transplantation compared with the liver treated with CCl_4 alone (I. Sakaida, unpublished data, 2003). As shown in Fig. 7, migrated BMCs seemed to reduce the fine network pattern of activated stellate cells. Thus, transplanted BMCs may affect activated stellate cells by reducing their number—*e.g.*, by leading them to apoptosis. However, further examinations are necessary to determine the exact relationship between BMCs and resident stellate cells.

Our recent data[12] indicated that the subpopulation of BMCs, nonhematopoietic cells in bone marrow, separated using an anti-Liv8 antibody, will transdifferentiate into hepatocytes in the liver damaged by CCl_4 induction. The present study clearly indicates that this subpopulation of BMCs is also responsible for the resolution of liver fibrosis (fibrolysis) induced by CCl_4 treatment.

In conclusion, the present study introduces a new concept for the treatment of liver fibrosis.

References

1. Petersen BE, Bowen WC, Patrene KD, Mars WM, Sullivan AK, Murase N, et al. Bone marrow as a potential source of hepatic oval cells. Science 1999;284:1168–1170.
2. Theise ND, Nimmakayalu M, Gardner R, Illei PB, Morgan G, Teperman L, et al. Liver from bone marrow in humans. HEPATOLOGY 2000;32:11–16.
3. Alison MR, Poulsom R, Jeffery R, Dhillon AP, Quaglia A, Jacob J, et al. Hepatocytes from nonhepatic adult stem cells. Nature 2000;406:257.
4. Krause DS, Theise ND, Collector MI, Henegariu O, Hwang S, Gardner R, et al. Multi-organ, multi-lineage engraftment by a single bone marrow-derived stem cell. Cell 2001;105:369–377.
5. Lagasse E, Connors H, Al-Dhalimy M, Reitsma M, Dohse M, Osborne L, et al. Purified hematopoietic stem cells can differentiate into hepatocytes in vivo. Nat Med 2000;6:1229–1234.

6. Orlic D, Kajstura J, Chimenti S, Jakoniuk I, Anderson SM, Li B, et al. Bone marrow cells regenerate infarcted myocardium. Nature 2001;410:701–705.
7. Korbling M, Katz RL, Khanna A, Ruifrok AC, Rondon G, Albitar M, et al. Hepatocytes and epithelial cells of donor origin in recipients of peripheral-blood stem cells. N Engl J Med 2002;346:738–746.
8. Okamoto R, Yajima T, Yamazaki M, Kanai T, Mukai M, Okamoto S, et al. Damaged epithelia regenerated by bone marrow-derived cells in the human gastrointestinal tract. Nat Med 2002;8:1011–1017.
9. Wagers AJ, Sherwood RI, Christensen JL, Weissman IL. Little evidence for developmental plasticity of adult hematopoietic stem cells. Science 2002;297:2256–2259.
10. Okabe M, Ikawa M, Kominami K, Nakanishi T, Nishimune Y. "Green mice" as a source of ubiquitous green cells. FEBS Lett 1997;407:313–319.
11. Terai S, Sakaida I, Yamamoto N, Omori K, Watanabe T, Ohata S, et al. An in vivo model for monitoring trans-differentiation of bone marrow cells into functional hepatocytes. J Biochem (Tokyo). 2003;134:551–558.
12. Yamamoto N, Terai S, Ohata S, Watanabe T, Omori K, Shinoda K, et al. A subpopulation of bone marrow cells depleted by a novel antibody, anti-Liv8, is useful for cell therapy to repair damaged liver. Biochem Biophys Res Commun 2004;313:1110–1118.
13. Watanabe T, Nakagawa K, Ohata S, Kitagawa D, Nishitai G, Seo J, et al. SEK1/MKK4-mediated SAPK/JNK signaling participates in embryonic hepatoblast proliferation via a pathway different from NF-kappaB-induced anti-apoptosis. Dev Biol 2002;250:332–347.
14. Sakaida I, Uchida K, Matsumura Y, Okita K. Interferon gamma treatment prevents procollagen gene expression without affecting transforming growth factor-beta1 expression in pig serum-induced rat liver fibrosis in vivo. J Hepatol 1998;28:471–479.
15. Sakaida I, Nagatomi A, Hironaka K, Uchida K, Okita K. Quantitative analysis of liver fibrosis and stellate cell changes in patients with chronic hepatitis C after interferon therapy. Am J Gastroenterol 1999;94:489–496.
16. Sakaida I, Tsuchiya M, Kawaguchi K, Kimura T, Terai S, Okita K. Herbal medicine Inchin-ko-to (TJ-135) prevents liver fibrosis and enzyme-altered lesions in rat liver cirrhosis induced by a choline-deficient L-amino acid-defined diet. J Hepatol 2003;38:762–769.
17. Sakaida I, Hironaka K, Uchida K, Suzuki C, Kayano K, Okita K. Fibrosis accelerates the development of enzyme-altered lesions in the rat liver. HEPATOLOGY 1998;28:1247–1252.
18. Jimenez MJ, Balbin M, Lopez JM, Alvarez J, Komori T, Lopez-Otin C. Collagenase 3 is a target of Cbfa1, a transcription factor of the runt gene family involved in bone formation. Mol Cell Biol 1999;19:4431–4442.
19. Nakada M, Nakamura H, Ikeda E, Fujimoto N, Yamashita J, Sato H, et al. Expression and tissue localization of membrane-type 1, 2, and 3 matrix metalloproteinases in human astrocytic tumors. Am J Pathol 1999;154:417–428.
20. Heissig B, Hattori K, Dias S, Friedrich M, Ferris B, Hackett NR, et al. Recruitment of stem and progenitor cells from the bone marrow niche requires MMP-9 mediated release of kit-ligand. Cell 2002;109:625–637.
21. Hattori K, Heissig B, Wu Y, Dias S, Tejada R, Ferris B, et al. Placental growth factor reconstitutes hematopoiesis by recruiting VEGFR1(+) stem cells from bone-marrow microenvironment. Nat Med 2003;8:841–849.
22. Tanaka A, Arai K, Kitamura Y, Matsuda H. Matrix metalloproteinase-9 production, a newly identified function of mast cell progenitors, is down-regulated by c-kit receptor activation. Blood 1999;94:2390–2395.
23. Baram D, Vaday GG, Salamon P, Drucker I, Hershkoviz R, Mekori YA. Human mast cells release metalloproteinase-9 on contact with activated T cells: juxtacrine regulation by TNF-alpha. J Immunol 2001;167:4008–4016.
24. Ohuchi E, Imai K, Fujii Y, Sato H, Seiki M, Okada Y. Membrane type 1 matrix metalloproteinase digests interstitial collagens and other extracellular matrix macromolecules. J Biol Chem 1997;272:2446–2451.
25. Kollet O, Shivtiel S, Chen YQ, Suriawinta J, Thung SN, Dabeva MD, et al. HGF, SDF-1, and MMP-9 are involved in stress-induced human CD34+ stem cell recruitment to the liver. J Clin Invest 2003;112:160–169.
26. Kanazawa Y, Verma IM. Little evidence of bone marrow-derived hepatocytes in the replacement of injured liver. Proc Natl Acad Sci U S A 2003;100(Suppl);11850–11853.
27. Forbes SJ, Russo FP, Rey V, Burra P, Rugge M, Wright NA, et al. A significant proportion of myofibroblasts are of bone marrow origin in human liver fibrosis. Gastroenterology 2004;126:955–963.

FEBS Letters 578 (2004) 10–20 FEBS 28981

Molecular signature associated with plasticity of bone marrow cell under persistent liver damage by self-organizing-map-based gene expression ☆

Kaoru Omori[a], Shuji Terai[a,*], Tsuyoshi Ishikawa[a], Kouji Aoyama[a], Isao Sakaida[a], Hiroshi Nishina[b], Koh Shinoda[c], Shunji Uchimura[d], Yoshihiko Hamamoto[d], Kiwamu Okita[a]

[a] *Department of Molecular Science and Applied Medicine (Gastroenterology and Hepatology), Yamaguchi University School of Medicine, Minami Kogushi 1-1-1, Ube, Yamaguchi 755 8505, Japan*

[b] *Department of Physiological Chemistry, Graduate School of Pharmaceutical Science, University of Tokyo, Hongo 7-3-1, Bunkyoku, Tokyo 113 0033, Japan*

[c] *Department of Neuroanatomy and Neuroscience, Yamaguchi University School of Medicine, Minami Kogushi 1-1-1, Ube, Yamaguchi 755 8505, Japan*

[d] *Department of Computer Science and Systems Engineering, Faculty of Engineering, Yamaguchi University, Tokiwadai 2-16-1, Ube, Yamaguchi 755 8505, Japan*

Received 22 April 2004; revised 3 September 2004; accepted 23 September 2004

Available online 2 November 2004

Edited by Gianni Cesareni

Abstract The mechanism that regulates the plasticity of bone marrow cells (BMCs) into hepatocytes is poorly understood. We developed a green fluorescent protein/carbon tetrachloride model to find that BMC transplantation recovered liver damage. Serum albumin level and liver fibrosis were recovered by BMC transplantation. To understand the mechanism, we used DNA-chip technology to profile the change of transient gene expression before and after BMC transplantation. On the basis of gene expression with self-organizing map using specific equation, genes were classified into 153 clusters. The information is useful to understand the dramatic gene activation during the process of the plasticity of BMC.

Keywords: Bone marrow cell; Plasticity; Regenerative Medicine; Gene expression; Microarray analysis; Self-organizing map; Liver regeneration

1. Introduction

Recently, several groups have reported the possible plasticity of bone marrow cells (BMC) to differentiate into a variety of non-hematopoietic cell lineages [1,2]. Ever since, the differentiation of BMC into hepatocytes in human was documented following a bone marrow transplantation from a man to a woman [3]. The mechanism of the plasticity of BMC was discussed whether that was occurred with cell fusion, nuclear reprogramming [4–6] or trans-differentiation [7,8]. We think both cell fusion and trans-differentiation might be important to understand the mechanism of BMC plasticity. On the other hand, in cardiovascular medicine, clinical research has been conducted to evaluate the use of BMCs in regenerating the myocardium and vessels, and some positive results have been obtained [9,10]. These findings suggest the usefulness of BMCs as the source of cells in developing the next-generation of treatment for liver regeneration [11]. We first tried to understand how we could use BMC to repair damaged liver. We have developed a model [named as a green fluorescent protein/carbon tetrachloride (GFP/CCl_4)] to evaluate the usefulness of BMC transplantation for damaged liver [12,13]. In this model, 0.5 ml/kg of carbon tetrachloride (CCl_4) is administered twice weekly to induce liver cirrhosis and then GFP-positive BMCs are transplanted through the causal vein [14]. Under continuous liver injury, immunostaining using anti-GFP antibodies [15] showed that GFP-positive BMCs migrated into the marginal area of the hepatic lobule starting from day 1 after BMC transplantation, and with time, while forming a hepatic cord towards the central vein, the distribution of GFP-positive BMCs expands [12,16]. Also, using Liv2, a hepatoblast-specific antibody that we developed [17], it has been shown that BMCs first trans-differentiate into Liv2-positive hepatoblasts and then differentiated into albumin-positive hepatocytes. Furthermore, the level of serum albumin significantly increases with time in recipient mice. Liver fibrosis induced by CCl_4 injection was recovered by BMC transplantation [18]. These findings suggest that this GFP/CCl_4 model can be used

☆ Grant Support: This study was supported by Grants-in-Aid for Scientific Research from the Japan Society for the Promotion of Science (Nos. 13470121, 13770262, 15790348, *16390211* and *16590597*) and for translational research from the Ministry of Health, Labor and Welfare (H-trans-5).

* Corresponding author. Fax: +81-836-222-240.
E-mail address: terais@yamaguchi-u.ac.jp (S. Terai).

Abbreviations: BMC, bone marrow cell; SOM, self-organizing map; CCl_4, carbon tetrachloride; EGFP, enhanced GFP; GFP, green fluorescent protein; RT, reverse transcriptase; HNF4-α, hepatocyte nuclear factor 4 alpha; VEGF, vascular endothelial growth factor; HGF, hepatocyte growth factor; FAH, fumarylacetoacetate hydrolase; TNFR, tumor necrosis factor receptor; FGF, fibroblast growth factor; MMP, matrix metalloproteinase; TIMP, tissue inhibitor of metalloproteinase; NumbL, Numblike; HOX, homeobox; GPI, glucose-6-phosphatase isomerase

0014-5793/$22.00 © 2004 Published by Elsevier B.V. on behalf of the Federation of European Biochemical Societies.
doi:10.1016/j.febslet.2004.09.090

to understand the process of plasticity of BMCs under persistent liver damage condition. It is important to understand what had happened in GFP/CCl_4 model after BMC transplantation in mRNA level. DNA chips are recently developed tools used in genetic analyses [19]. While it is possible to obtain genetic data using DNA chips, the vast amount of information collected makes it difficult to precisely interpret the factors involved in the gene expression. Therefore, in the present study, patterns of global gene expression at different times were compared between mice with BMC transplantation and those without. Self-organizing map (SOM) is a statistical technique that has been recently used in analyzing microarray data and, via this method, it is possible to visualize a vast amount of complicated and multidimensional data [20]. In this analysis, we made a specific equation to extract genes with expressions that altered in relation to BMC transplantation. Here, we present the results obtained from this study.

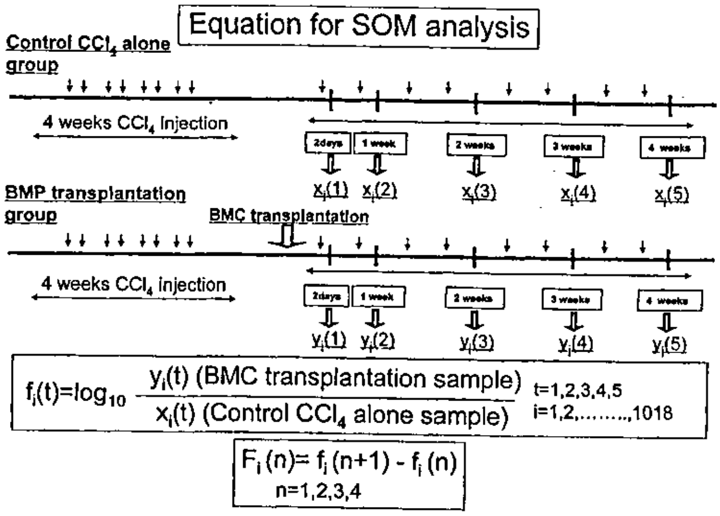

Fig. 1. Defined equation in this analysis. (↓) Arrow indicates CCl_4 injection twice a week in GFP/CCl_4 model. We analyzed gene expression in each time point (2 days, 1 week, 2 weeks, 3 weeks, and 4 weeks). $y_i(t)$ showed the gene expression level of the liver after BMC transplantation. $x_i(t)$ showed the gene expression level of the liver CCl_4 alone injection group. We define $f_i(t)$: $f_i(t) = \log_{10} y_i(t)/x_i(t)$. By using this, we succeeded in extracting the change of gene expression by BMC transplantation. We are interested in following the change of the values of $F_i(t) = f_i(t+1) - f_i(t)$ with the increase in t.

Table 1
Lists of primers for selected 13 genes

Cluster	Gene name (Accession No.)	Primer – forward (5′–3′) Primer – reverse (5′–3′)	Target	Tm
86	c-kit (NM02099)	TCCAACGATGTGGGCAAGAG AATGAGCAGCGGCGTGAA	90	55
86	FGP6 (M92415)	CATGGTCTATACCGGCCACA GGCTGCTGACATGAAACCAAAG	88	63
125	MMP2 (NM008610)	CCCTGATGTCCAGCAAGTAGATG ATTCCAGGAGTCTGCGATGAG	148	62
125	MMP9 (NM013599)	ACGACATAGACGGCATCCAGTA TCGGCTGTGGTTCAGTTGTG	90	53
92	TIMP2 (NM011594)	ACACGCTTAGCATCACCCAGA TGTGACCCAGTCCATCCAGAG	137	63
13	HGF (NM010427)	CCCAAACATCCGAGTTGGCTAC TTCCCATTGCCACGATAACA	84	63
1	NumbL (NM010950)	TATGCAGCCTCCGTTTGTG GCGTTGGCTACCATCTGTGAA	102	62
1	HOXD3 (NM010468)	CCATAAATCAGCCGCAAGGA GGATGGGTCGAGGACTTACCTTAG	112	63
152	GPI (NM008155)	TGGACGGCAAAGATGTGATG CGATGTTGATGATGTCCGTGA	129	63
152	VEGF (NM009505)	ATGCGGATCAAACCTCACCA CCGCTCTGAACAAGGCTCAC	129	63
136	TNFR1 (NM011609)	CTGCTCTACGAATCACTCTGCTC ACAGCATACAGAATCGCAAGGTC	113	62
151	HNF4 (NM008261)	CCAAGTACATCCCGGCCTTC CTAGGAGCAGCACGTCCTTAAAC	132	62
151	FGF2 (NM008006)	GGCTGCTGGCTTCTAAGTGTG ACTGCCCAGTTCGTTTCAGTG	129	62

2. Materials and methods

2.1. Experimental protocol (GFP/CCl_4 model)

We developed a new in vivo model in which we could monitor the plasticity of BMCs into hepatocytes [12,16]. The mouse line C57BL6/Tg14 (act-EGFP) OsbY01 was a kind gift from Dr. Masaru Okabe (Genome Research Center, Osaka University, Osaka, Japan) [14]. C57BL/6 female mice were purchased from Japan SLC (Shizuoka, Japan). We injected 0.5 ml/kg body weight of CCl_4 into C57BL/6 mice at 6 weeks of age via the peritoneum twice a week for 4 weeks to induce persistent liver damage. At this time, the condition of recipient mice was liver cirrhosis. One day after 4 weeks of CCl_4 injection, 1×10^5 GFP-positive BMCs were injected slowly using a 31 G needle and Hamilton syringe via the tail vein. The mice that were injected with CCl_4 only were used as the control group. After BMC transplantation, the same dose of CCl_4 was injected twice a week. Individual mice were killed at 18 h after initial CCl_4 injection (2 days after BMC transplantation) and once a week after BMC transplantation for 4 weeks. All processes including surgical steps confirmed to the guidance of Yamaguchi University for animal and recombinant DNA experiments.

2.2. RNA preparation and microarray analysis

In both the BMC transplantation and control groups, the liver was excised 2 days and 1, 2, 3, and 4 weeks after transplantation. The mice were killed by cervical dislocation. The whole liver was removed and immediately frozen in liquid nitrogen. Liver samples were pooled at least two from whole liver of both mice groups (BMC transplantation and control CCl_4 damage at each points). Total RNA was isolated from pooled liver samples using an Atlas Glass Total RNA Isolation Kit (Clontech, Palo Alto, CA) [21]. Single strands of cDNA were synthesized using the primer mix, dNTP, aminoacryl dUTP, and MMLV-RT using an Atlas Glass Fluorescent Labeling Kit (Clontech). The synthesized cDNA probes were coupled to monoreactive Cy3 for fluorescent labeling. Probes were prepared in the same manner for the control group (no BMC transplantation) and BMC transplantaion group at the same time. The DNA microarray analysis was conducted using an Atlas Glass Mouse 1.0K Microarray System (Clontech) [22]. The above-mentioned cDNA probes were hybridized to a DNA chip composed of about 1100 DNA fragments by incubating the chip overnight at 50 °C with the probe. After incubation, the chip was washed using GlassHyb Wash Solution, RNase water and 20× SSC, rinsed with distilled water and then air dried. The signal intensity of each gene was measured using a fluorescent scanner (Axon Instruments, CA). The spot intensity of expression of each gene was assessed using the ArrayGauge System (Fuji Film, Tokyo, Japan). The raw data of the spot intesity were used for SOM analysis (All raw data of microarray are available at http://liver-project.med.yamaguchi-u.ac.jp/research/). We performed several analyses to obtain representative data.

2.3. SOM analysis for microarray

The microarray analysis showed that, of the 1100 genes on the DNA chips, although the expression of some genes was too small for further analysis, the expression data recorded of the remaining 1018 genes were sufficient for SOM data analysis. At each of five sampling times, i.e., 2 days and each week for 4 weeks, expression levels of 1018 genes for both control CCl_4 damage and BMC transplantation group were measured, respectively. To extract the genes that are differentially expressed before and after BMC transplantation, we defined the following equation (Fig. 1):

$$f_i(t) = \log_{10} \frac{y_i(t)}{x_i(t)}, \quad t = 1, 2, 3, 4, 5, \quad i = 1, 2, \ldots, 1018 \qquad (1)$$

where $x_i(t)$ is the expression level of the control CCl_4 alone sample (CCl_4 alone without BMC transplantation) and $y_i(t)$ is the expression level of BMC transplantation sample for gene i (1,2,…,1018) at sampling point t, respectively. The term $f_i(t)$ represents the expression level of GFP/CCl_4 group normalized by the control group. If $y_i(t) = x_i(t)$, at that the value of $f_i(t)$, i.e., $\log_{10} 1$, was zero. By using this, we succeeded in extracting the change of gene expression by BMC transplantation. Point t shows time. t = 2d, 1w, 2w, 3w, and 4w showed 1, 2, 3, 4, and 5, respectively. To extract the change of gene expression with time, we followed the change of the values of $f_i(t+1) - f_i(t)$ with the increase in t. Using $f_i(t)$, we defined the 4-dimensional vector $F_i = [F_i(1), F_i(2), F_i(3), F_i(4)]^T$ for gene i, where

$$F_i(1) = f_i(2) - f_i(1)$$
$$F_i(2) = f_i(3) - f_i(2)$$
$$F_i(3) = f_i(4) - f_i(3)$$
$$F_i(4) = f_i(5) - f_i(4)$$

All genes were described and then used as input patterns for SOM analysis. SOM was performed using the SOM toolbox in MATLAB (The Mathworks Inc., Natick, MA; and http://www.cis.hut.fi/projects/somtoolbox/).

Each element of these vectors $[Fi(i = 1,2,3,\ldots,1018)]$ represents a chronological change of gene expression after BMC transplantation in GFP/CCl_4 model.

2.4. Reverse transcriptase (RT)-PCR analysis

Total RNA was isolated from the whole liver of both mice groups (BMC transplantation and control CCl_4 damage (n = 2, each group) using Isogen Total-RNA isolation kit (Nippon Gene Co., Ltd., Tokyo, Japan) at each of five sampling times, i.e., 2 days and each week for 4 weeks. These samples were obtained by independent experiments from microarray analysis. RT step was performed using SYBR RT-PCR kit (Takara Co., Tokyo, Japan).

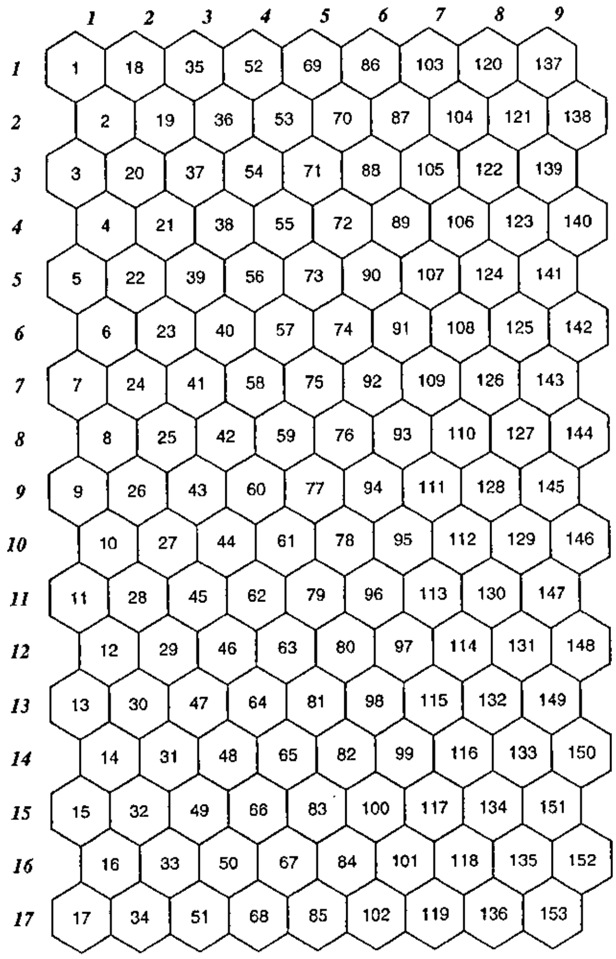

Fig. 2. The 1018 genes analyzed using microarray were divided into 153 clusters and arranged in a 17 × 9 matrix (height × width) of 153 hexagons (all raw data of microarray are available at http://liver-project.med.yamaguchi-u.ac.jp/research/). The number of genes varied among the clusters. Clusters with similar elements were arranged close to each other in the matrix.

Two μl of cDNA solution (100 ng of initial RNA) was amplified in 20 μl of reaction mixture containing 5 pmol of forward and reverse primer. PCR was performed for a total of 45 cycles, each of 95 °C for 5 s and 60 °C for 20 s [23]. We selected 13 genes to further clarify the difference expression pattern of each gene. c-kit, fibroblast growth factor (FGF)-6, matrix metalloproteinase (MMP)-2, MMP-9, tissue inhibitor of metalloproteinase (TIMP)-2, Hepatocyte growth factor (HGF), Numblike (NumbL) and homeobox (HOX) D3, Glucose-6-phosphatase isomerase (GPI), vascular endothelial growth factor (VEGF), tumor necrosis factor receptor (TNFR)-1, hepatocyte nuclear factor (HNF)-4 and FGF-2 were selected. The primer used in this study is shown in Table 1. The relative ratio of each gene expression was determined referring with the mean expression level of control house keeping gene, glyceraldehyde-3-phosphate dehydrogenase (GAPDH) and 18 S ribosomal RNA expression.

2.5. SOM analysis compared between RT-PCR and microarray

To validate the results of SOM analysis depend on microarray, we compared SOM analysis between microarray and RT-PCR. We used the same equation and performed SOM analysis (Fig. 1) based on both the data of RT-PCR and microarray.

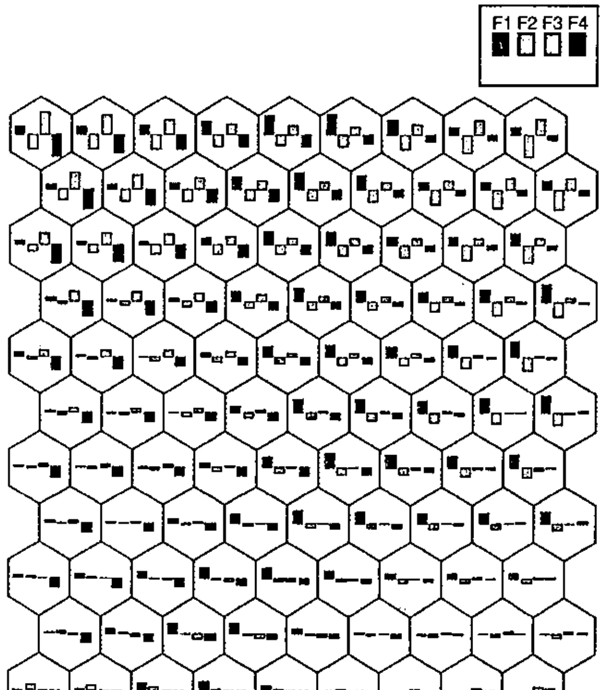

Fig. 3. The median value for gene expression for *F1*, *F2*, *F3*, and *F4* in each cluster is presented as a bar chart. As a reference, in cluster 1, the median value in *F1* and *F3* was increased, while that in *F2* and *F4* was decreased.

3. Results

The 1018 genes that could be analyzed by the DNA chips were classified into 153 clusters by SOM (Fig. 2). Genes in the same cluster showed similar gene expression pattern during the process of BMC trans-differentiation. On the SOM matrix, clusters with similar vector F_i elements (*F1*–*F4*) were arranged in close proximity to each other. Therefore, adjacent clusters on the matrix exhibited similar chronological changes in gene expression profiles during the process of plasticity of BMC into hepatocyte. Fig. 3 shows bar charts that represent the median value of gene expression for each cluster in *F1*, *F2*, *F3*, and *F4*. By analyzing each element (*F1*–*F4*) of vector *Fi*, the clusters were color coded to aid visualization of the SOM data (Fig. 4). For example, in the *F1* output, clusters 69, 70, and 86 containing upregulated genes in *F1* were colored dark brown. On the other hand, clusters with downregulated genes in *F1* were colored dark blue. The color bar on the right-hand side of the figure indicates the degree of gene expression from *F1* to *F4*, and a value of 0 indicates that there was little transient change in gene expression between the BMC transplantation and control CCl_4 injection groups. The following clusters exhibited marked changes in transient gene expression: in *F1*, clusters 69, 70, 86, 92, 125, 140, 141, 142, and 143; in *F2*, clusters 13, 14, 15, 16, 17, 32, 33, and 34; in *F3*, clusters 1, 2, 18, and 137; and in *F4*, clusters 118, 119, 133, 134, 135, 136, 148, 149, 150, 151, 152, and 153. To validate the data of SOM analysis based on microarray analysis, we performed SOM

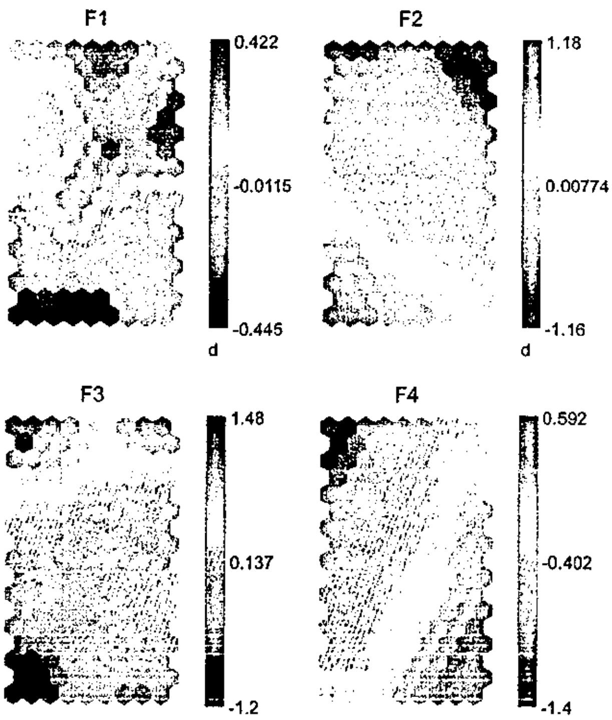

Fig. 4. The clusters were color-coded based on the median values for gene expression at the *F1*, *F2*, *F3*, and *F4* time periods. The color bar on the right hand side indicates the values in each period; dark brown for upregulated and dark blue for downregulated. A value of 0 indicates that there was little chronological change in gene expression between the transplantation and control groups.

analysis based on the data of RT-PCR for selected 13 genes using the same equation (Figs. 5A and B). Table 2 shows the list of genes in each cluster.

4. Discussion

By using specific equation to extract change of gene expression after BMC transplantation, we found that there were dramatic changes for both gene expression and distribution of gene clusters after BMC transplantation in GFP/CCl_4 model (Figs. 3 and 4). 1018 genes were classified into 153 patterns of change of gene expression using SOM analysis. These results might show that many genes had important reciprocal roles during the process of differentiation of BMC into albumin positive hepatocyte. To validate the SOM analysis based on microarray analysis, we performed SOM analysis based on selected 13 gene expressions analyzed by RT-PCR independently. c-kit, FGF6, MMP2, MMP9, and TIMP2 were selected from serious clusters at *F1* periods (clusters 86, 92, and 125). HGF was selected from *F2* periods (cluster 13). NumbL and HOXD3 were selected from *F3* (cluster 1). GPI, VEGF, TNFR1, HNF4, and FGF2 were selected from *F4* (clusters 136, 151, and 152). As shown in Fig. 5, we found the similar position of these selected genes. This means that the change of gene expression from microarray analysis is similar to that from RT-PCR analysis. These results showed the consistency of SOM analysis based on microarray using specific equation.

Cluster with color deeper than dark orange (69, 70, 125, 141, 142, and 143) showed the dramatic change in *F1* period (Fig. 4). The c-kit gene, which was present in cluster 86, encodes a stem cell factor receptor which is related with rat hepatic stem cell, oval cell, activation [24]. FGF-6 was also extracted in cluster 86. FGF was known to have an important role of hepatocyte proliferation and liver development [25]. To focus on the change of *F1* to *F4* in cluster 86, we found that genes in cluster 86 were upregulated soon after BMC transplantation suggesting that the expression of these genes changes dynamically and might have an important role in the early stage of plasticity of BMC (Fig. 3). In cluster 125, genes involved in the regulation of liver fibrosis such as MMP2 and MMP9 were pointed out. These results were consistent with liver fibrosis recovered by BMC transplantation. MMP9 has been reported to facilitate the induction of hematopoietic cells from the marrow via the kit signal transduction pathway [26]. This result might suggest that ECM might be important for the

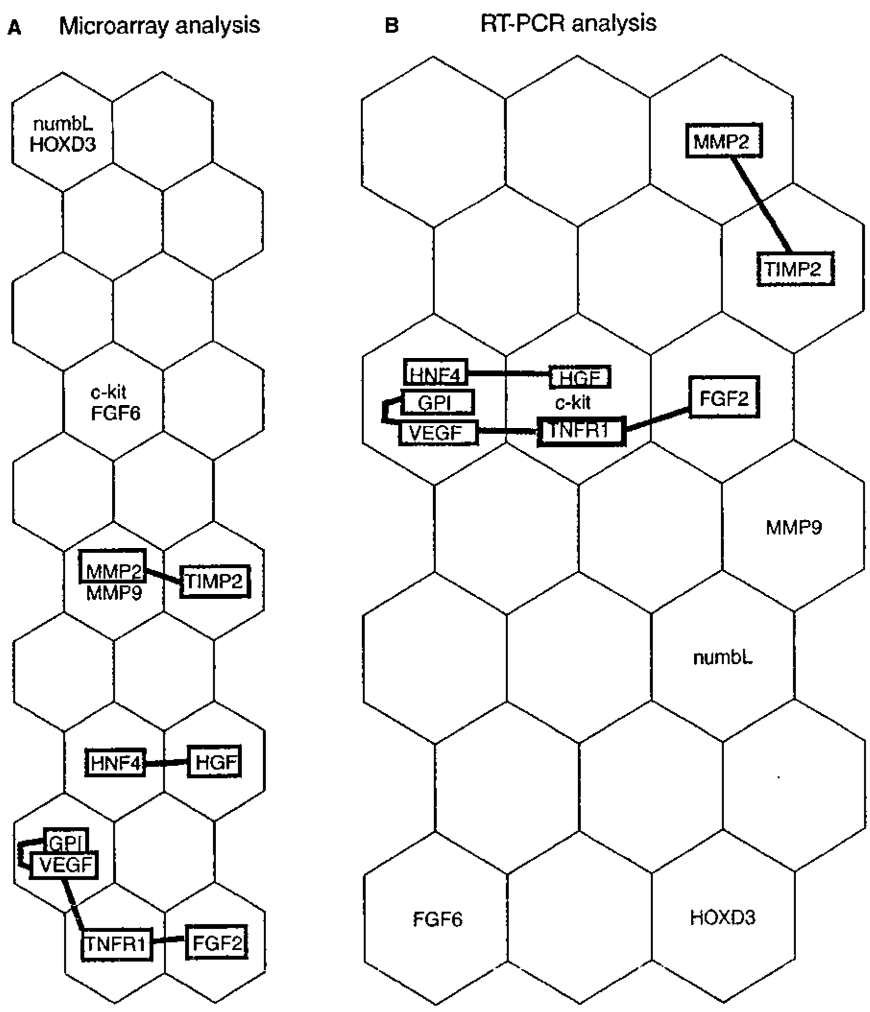

Fig. 5. For the genes, the data of microarray (A) and RT-PCR (B) were classified into clusters by SOM, respectively. Clusters with similar elements were arranged close to each other in the matrix.

Table 2
Selected *gene* grouped to clusters

Cluster No.	GenBank ID	Gene description
Clusters with remarkable variation of gene expression in F1		
86	U52951	Enhancer of zeste homolog 2 (EZH2); ENX1H
	X06368 X68932	Macrophage colony-stimulating factor 1 receptor (CSF1R) c-fms proto-oncogene
	Y00864 NM02099	c-kit proto-oncogene
	U14173	ski proto-oncogene
	M92415	Fibroblast growth factor 6 (FGF6)
69	X07439	Homeobox protein 3.1 (HOX3.1)
	X57487	Paired box protein 8 (PAX8)
	U43788	POU domain class 2-associating factor 1 (POU2AF1); OCT-binding factor 1 (OBF1); BOB1; OCA-B
	M84819	Retinoic acid receptor-γ (RXR-γ; RXRG)
	AF015848	E2F transcription factor 3 (E2F3)
	Z22649	mpl proto-oncogene; thrombopoietin receptor
	L27105	MOESIN-ezin-radin-like protein (MERLIN); schwannomin (SCH); neurofibromatosis 2(NF2)
	U51196	EB1 APC-binding protein
	Y00671	met proto-oncogene
	Z12604	Matrix metalloproteinase 11 (MMP11); stromelysin 3 (STMY3)
70	D90156	Myogenin (MYOG); myoD1-related protein
	U51037	CCCTC-binding factor (CTCF)
	U06119	Cathepsin H
142	J04946	Angiotensin-converting enzyme (ACE); dipeptidyl carboxypeptidase I (DCP1); kinase II
	U10551	Gem induced immediate early protein
	L34290	Transducin β-5 subunit GTP-binding protein G(i)/G(s)/G(t) β subunit 3
	M96653	Adenylate cyctase 6
	Z71173	Inositol 1,4,5-triphosphate receptor 2
	L76946	Phosphodiesterase 1C
	U12919	Adenylate cyclase type VII (AIP pyrophosphate-lyase) (adenylyl cyclase) (KIAA0037)
	D31788	BP3 alloantigen
	AA000715	S100 calcium-binding protein A1; S-100 protein α chain
	U97327	Calcylin binding protein
	U73004	Antileukoproteinase 1 (ALP1); secretory leukocyte protease inhibitor
140	U58992	Mothers against decapentaplegic homolog 1 (MADH1; mSMAD1); TGF-β signaling protein 1
	U36203	snoN: ski-related oncogene
	D17571	NADPH-cytochrome P450 reductase (CPR); POR
	U68058	Secreted frizzled-related protein 3 (SFRP3; mFIZ); frezzled
	U77638	Mothers against dpp homolog 5 (SMAD5; MADH5)
	M33385	Neurotrophic tyrosine kinase receptor type 2 (NTRK): tyrosine kinase receptor B (TRKB)
	X57277	ras-related C3 botulinum substrate 1 (RAC1)
	M21531	Calbindin-28K: calbindin 1 (CALB1)
	U53142	Nitric oxide synthase 3, endothelial cell
	U37775	Tuberin: TSC2 (tuberous sclerosis 2 protein)
	J05261	Lysosomal protective protein; cathepsin A; carboxypeptidase C (CPC); MO54
	M81591	Membrane metallo endopeptidase
	M14222	Cathepsin B (CTSB)
	X15475	Peripherin (PRPH)
141	U61969	Wingless-related MMTV integration site 10a protein (WNT10A)
	X76292	Desert hedgehog homolog (DHH); HHG3
	X67962	Interleukin 7 (IL7)
	X66196	Recoverin (RCV1; RCVRN); cancer-associated retinopathy protein (CAR protein), 23-kDa photoreoeptor cell-specific protein
	U57311	14-3-3 protein η; protein kinase C inhibitor protein 1 (KCIP1); tyrosine 3-monooxygenase/tryptophan 5-monooxygenase activation protein η polypeptide (YWHAH)
	X16490	Macrophage plasminogen activator inhibitor 2 (PAI2; PLANH2)
	X05211	Laminin γ 1 subunit (LAMC1); laminin B2 subunit
125	U03421	Interleukin 11 (IL11)
	M84324	Matrix metalloproteinase 2 (MMP2)
	NM008610	
	X72795	Matrix metalloproteinase 9 (MMP9)
	NM013599	
	M59470	Cystatin C; cystatin 3 (CST3)

(*continued on next page*)

Table 2 (*continued*)

Cluster No.	GenBank ID	Gene description
143	U94350	Radical fringe homolog (RFNG)
	U37720	Cell division cycle 42 homolog (CDC42); 25-kDa GTP-binding protein (G25K)
	X73985	Calbindin 2 (CALB2); calretinin
	X61432	Calmodulin (CALM; CAM)
	U48853	ork-associated substrate (CRKAS; CAS)
	U24680	Dishevelled 2 homolog (DVL2)
	D00611	Basic immunoglobulin superfamily (BASIGIN; BSG); membrane glycoprotein 42 (GP42), neurothelin; CD147 antigen
	M28730	Tubulin β 4 (TUBB4)
	Z21848	DNA polymerase δ catalytic subunit (POLD1)
92	U37331	T-box protein 6 (TBX6)
	M61909	relA proto-oncogene; NF-κ-B transcription factor p65 subunit (NF-κB p65)
	U18542	Calcitonin receptor 1b
	U17985	Cannabinoid receptor 1 (CNR1; CBR), brain cannabinoid receptor
	U41285	Segment polarity protein dishevelled homolog 3 (DVL3), DSH homolog 3
	X62622	Tissue inhibitor of metalloproteinase 2 (TIMP2)
	NM011594	
	L07803	Thrombospondin 2 (THBS2; TSP2)
	X53929	Decorin (DCN); bone proteoglycan II (PG-S2), PG40
	X61435	Neuronal kinesin heavy chain (NKHC); KIF5C
	D10061	DNA topoisomerase I (*TopI*)
	D28492	Caspase 2 (CASP2); NEDD2 protein; ICH1 cysteine protease
	X66323	X-ray repair-complementing defective repair in Chinese hamster cells 5 (XRCO5)
Clusters with remarkable variation of gene expression in F2		
17	AF017085	BAP-135 homolog; DIWSIT; general transcription factor II-I (GTF2I)
	U77969	Neuronal PAS domain protein 2
	X97817	Semaphorin F(SEMAF)
	M84487	Vascular cell adhesion molecule 1 (VCAM1)
	M59378	Tumor necrosis factor receptor superfamily member 1B2 (TNFRSF1B2); tumor necrosis factor receptor 2 (TNFR2)
	U25995	Receptor (TNFRSF)-interacting serine-threonine protein kinase 1 (RIPK1; RIP)
	L22472	BCL2-associated X protein membrane isoform alpha (BAX-alpha)
	L33406	Uromodulin
	AF007268	Fibroblast growth factor 15 (FGF15)
	AF030433	Dickkopf homolog 1 (mDKK1)
	AF031896	Cerberus-related protein1 (CERR1)
	X58995	Calcium/calmodulin-dependent protein kinase IV catalytic subunit (CAM kinase-CR; CAMKIV;
34	D32132	Hairy and enhancer of split protein 5 (HES5)
	Z93947	Semaphorin H (SEMAH)
	U69535	Semaphorin J (SEMAJ)
	X97818	Semaphorin G (SEMAG); SEMA5B
	U25416	Tumor necrosis factor receptor superfamily member 8 (TNFRSF8); CD30L receptor
	U39643	fas-associated factor 1 (FAF1)
	Z22703	Fibroblast growth factor 7 (FGF7)
	X63615	Calcium/calmodulin-dependent protein kinase type II β subunit (CAM-kinase II β; CAMK-II β)
	U43187	Mitogen-activated protein kinase kinase kinase 3 (MAPKKK3; MAP3K3; MAPK/ERK kinase kinase 3 (MEK kinase 3; MEKK3)
	L35236	Mitogen-activated protein kinase 10 (MAP kinase 10 MAPK10; PRKM10); MAP kinase p49 3F12; Stress-activated o-jun N-terminal kinase 3 (JNK3); SAPK/ERK kinase 2 (SERK2)
	U03856	Receptor-type protein tyrosine phosphatase (PTPRCAP); C polypeptide-associated protein; CD45-Associated protein (C045-AP), LSM
16	L20331	Adenosine A3 receptor
	L41145	Bone morphogenetic protein 5 (BMP5)
	AB006787	Mitogen-activated protein kinase kinase kinase 5 (MAPKKK5; MAP3K5); MAPK/ERK kinase kinase S (MEKK5); apoptosis signar-regulating kinase 1 (ASK1)
	U92456	Serine/aninine-rich protein specific kinase 2 (SRPK2), WW domain binding protein 6 (WBP6)
15	X81579	Insulin-like growth factor-binding protein 1 (IGF-binding protein 1; K3FBP1)
	U60530	Mothers against decapentaplegic homolog 2 (MADH2; mSMAD2)
	AB005141	Klotho protein (KL)
	U77039	Four and a half LM domains 1 (FLH1); KyoT
51	Z32675	Hairless protein (HR)
	L10075	DNA-binding protein SMBP2
	S56660	Retinoic acid receptor β (RAR-β; RARB); nuclear receptor subfamily 1 group B member 2

Table 2 (*continued*)

Cluster No.	GenBank ID	Gene description
	X57413	Transforming growth factor β 2 (TQF-beta 2; TOFB2)
	M20473	cAMP-dependent protein kinase type I β regulatory chain (PRKAR1B)
	Y00703	Guanine nuclaotide-binding protein alpha stimulating activity potypeptide (GNAS)
32	Y07836	Stimulated by retinoic acid protein 14 (STRA14); STRA13; E47 interaction protein 1 (EIP1)
	X85993	Collapsin 1; semaphorin IIIA (SEMA3A), SEMAD
	L28177	Growth arrest and DNA damage-inducible protein (GADD45), DNA damage-inducible transcript 1
	L33768	Janus tyrosine-protein kinase 3 (JAK3)
	U07617	Growth factor receptor-bound protein 2 (GRB2); ASH protein
	L02526	Mitogen-activated protein kinase kinase 1 (MAP kinase kinase 1; MAPKK1; MAP2K1; PRKMK1); MAPK/ERK kinase 1 (MEK1)
	U66058	DNA ligase III; polydeoxyribonucleotide synthase (ATP) (DNL3)
	L28819	Involucrin (IVL)
33	X97052	Mitogen-activated protein kinase kinase 6 (MAP kinase kinase 6; MAPKK6; MAP2K6; PRKMK6); MAPK/ERK kinase 6 (MEK6); SAPKK3
	L09562	Protein-tyrosine phosphatase γ (R-PTP- γ; PTPRG)
	Z32767	DNA damage repair & recombination protein 52 homolog (RAD52)
14	X81466	Ephrin type A receptor 7 (eph receptor A7; EPHA7), embryonic brain receptor tyrosine kinase (EBK); developmental kinase 1 (mDK1)
	U37522	Tumor necrosis factor superfamily member 10 (TNFSFK 10); TNF-related apoptosis inducing ligand
	D38258	Fibroblast growth factor 9
	X77113	Growth differentiation factor 9 (GDF9)
	X06381	Leukemia inhibitory factor (LIF); cholinergic differentiation factor
	Z22532	Syndecan 1 (SYND1)
	M75716	Alpha-1-antitrypsin, 1-2 (AAT2), serine proteinase inhibitor 1-2 (SPI1-2); alpha 1 protease inhibitor 2; alpha-1- antiproteinase
	M64292	Anti-protiferative B-cell translocation gene 2 (BTG2); NGF- inducible protein TIS21
	L23971	Fragile X mental retardation syndrome 1 homolog (FMR1; FMRP)
13	U95610	NIMA-related protein kinase 2 (NEK2)
	U05252	Special AT-rich sequence-binding protein 1 (SATB1)
	U70017	Cyclin-D binding Myb-like protein (hDMPI)
	AF001287	Neural cell adhesion molecule 2 (NCAM2), olfactory axon cell adhesion molecule (OCAM)
	J04806	Osteopontin (OP); bone sialoprotein 1; minopontin; early T-lymphocyte activation 1 protein (ETA1); secreted phosphoprotein 1 (SPP1), calcium oxalate crystal growth inhibitor protein
	X83930	Cadherin 5 (CDH5); vascular epithelial cadherin (VE-cadherin)
	AF003747	Zinc transporter 4 (ZNT4)
	M16472	Myelin proteolipid protein (PLP). lipophilin; DM20
	X15830	7B2 neuroendrocrine protein: secretogranin V (SGV; SCG5)
	X72307 NM010427	Hepatocyte growth factor (HGF)
	D84372	Non-receptor type II protein cyrosome, phosphocyrosome phosphrase
	M38700	ATP-dependent DNA helicase II 70-kDa subunit 70-kDa thyroid autoantigen; lupus Ku autoantigen protein p70 CTC box-binding factor 75-kDa subunit (CTCBF; CTC75)
cluster with remarkable variation of gene expression in F3		
1	UB6441 NM010950	numfaiike (numbL; m-nbl)
	M33158	CD3 antigen zeta (CD3Z)
	X04648	Low-affinity IgG Fc receptor II β (FCGR2B)
	D49658	LIM-homeodomain protein L3; LHX8
	L12705	Engrailed protein (En-2) homolog
	D49474	SRY-box containing gene 17 (SOX17)
	X73573	Homeobox protein D3 (HOXD3)
	NM010468	
	U62522	Sp4 zinc finger transcription factor
	U25096	Lung Kruppel like factor (LKLF)
	X90329	Lbx 1 transcription factor
	X61753	Heat shook factor 1
	U53925	Transcription factor C1
	U97076	FLICE-like inhibitory protein long form (FLIP-L)
18	M55512	WT1; Wilms tumor protein; tumor suppressor
	M16449	Myeloblastosis prato-oncogene (MYB)
	X13945	Lung carcinoma myc-related oncogene 1 (L-myc; mycL1)
	M26391	Retinoblastoma-associated protein 1 (RB1); phosphoprotein 105 (PP105)
	U65594	Breast cancer type 2 susceptibility protein (BRCA2)
	U04807	FMS-like tyrosine kinase 3 ligand (FLT3L)
	M34563	T-ceB-specific surface glycoprotein CD28

(*continued on next page*)

Table 2 (*continued*)

Cluster No.	GenBank ID	Gene description
2	M32240	Peripheral myelin protein 22 (PMP22); CD25 antigen; SR13 myelin protein
	M63801	Gap junction alpha 1 protein (GJA1), connexin 43 (CXN43; CX43)
	AF013282	T-box protein 15 (TBX15); TBX14; TBX8
	U63386	Early development regulator 1 (EDR1); pdyhomeotic 1 homolog (mPH1)
	J05154	Lecithin cholesterol acyltransferase (LCAT); phosphatidylcholine sterot acyltransferase; phospholipid cholesterol acyftransferase
137	M55171	Rhodopsin (RHO), opsin (mOPS)
	D50311	Myocyte enhancer factor 2B (MEF2B)
	X14943	Contactin 1 (CNTN1); F3 neuronal cell adhesion molecule (F3CAM)
	U12570	von Hippel-Lindau syndrome homolog (VHLH)
	V00727	fos proto-oncogene
	U36799	retinoblastoma- like protein 2 (RSL2); retinoblastoma-relatad protein PRB2/p130
	S59388	Erythropoietin receptor (EPOR)
	Z31683	activin A receptor type IB
	S53216	Tyrosine-protein kinase ryk; kinase vik; nyk-R
	AF039601	TGF-bttta receptor type IB (betaglycan); candidate tumor suppressor gene
	X06203	Interleukin 8 (IL6)
Clusters with remarkable variation of gene expression in F4		
152	L12140	Groucho gene-related protein (GRG); amino enhancer of split protein (AES)
	M98502	Zinc finger protein 46
	S79463	Semaphorin I (SEMAI)
	X91144	P-selectin glycoprotein ligand 1 (PSGL1: SELPLG; SELP1)
	U04294	Electocardiographic QT syndrome 2 potassium channel subunit
	M14220	Glucose-6-phosphate isomerase (GPI)
	NM008155	
	M95200	Vascular endothelial growth factor (VEGF)
	NM009505	
	M30643	Heparin-fainding growth factor 5 (HBGF5); fibroblast growth factor 5 (FGF5)
	U51866 U17112	Casein kinase II alpha 1 related sequence 4 (CSNK2A1-RS4)
	U67916	Dentin sialophosphoprotein (DSPP)
	U49739	Unconventional myosin VI
153	S663B5	CREB-binding protein
	X85994	Semaphorin IIIC (SEMA3C); SEMAE
	U28724	Postmeiotic segregation increased 2 homolog (PMS2)
135	X12875	Neural cell adhesion molecule LI (N-CAM LI; LtCAM; CAML1)
	L24755	Bone morphogenetic protein 1 (BMP1)
	X83106	MAX dimerization protein (MAD)
	U34960	Transducin beta-2 subunit
	D86726	MCM6 DMA replication licensing factor (P105MCM)
136	D31967	Jumonji protein
	U59496	Hypoxia inducible factor 1 alpha subunit (HIF1-alpha; HIF1A); ARNT-interactmg protein
	X85992	Somaphorin C (SEMAC)
	X07640	Cell surface glycoprotein MAC-1 alpha subunit; CR-3 alpha subunit; GD11B antigen; leukocyte adhesion receptor MO1; integrin alpha-M (ITGAM)
	X57796	Tumor necrosis factor receptor 1 (TNFR1)
	NM011609	
	X53798	Small inducible cytokine subfampy B member 2 (SCYB2); macrophage inflamatory protein 2 (MIP2)
	X78850	Mitogen actived kinase-activated protein kinase 2 (MAPKAP kinase 2; MAPKAPK2); 60-kDa ribosomal protein S6 kinase potypeptide 1 (RPS6KC1)
	U43144	Phospholipase C β 3 (PLC-β 3; PLCB3)
	X83536	Matrix metalloproteinase 14 (MMP14): membrane-type matrix matatoproteinase I (MTMMP1)
	Y13602	Filensin, beaded filament structural protein in lens 1 (BFSP1)
150	AF033011	distal-less homeobox protein 5 (DLX5)
	D63644	Aryl hydrocarbon receptor nuclear translocator 2 (ARNT2)
	S70632 S70756	
	S70629	T-cell leukemia homeobox 1 (TLX1); homeobox protein 11 (HOX11)
	S81932	distal-less homeobox protein 3 (DLX3)
	X75330	Drosophila NK5 transcription factor-related locus 1 (NKX-5.1), H6 homeobox protein 3 (HMX3)
	U89487 U89489	LIM homeobox protein cofactor 1A (CUM1A); CUM1B; LIM domain-binding protein 3 (LDB3)
	U36340	CACCC-box-binding protein basic Kruppel like factor (BKLF): Kruppel-like factor 3 (KLF3)
	U42554	Single-minded 2 (SIM2)
	U33626	Promyelocytic leukemia gene (PML)

Table 2 (*continued*)

Cluster No.	GenBank ID	Gene description
	X56135	Prothymosin alpha (PTMA)
	U43512	Dystroglycan 1
	M13071	A-raf proto-oncogene
	M36829	Heat shock 84-kDa protein 1 (HSP84-1); HSP90
	M89802	Wingless-related MMTV integration site 7b protein (WNT7B)
	M30903	B-lymphocyte kinase (BLX)
	U43298	Laminin β 3 subunit (LAMB3); kalinin B1 subunit
151	D29015	Hepatic nuclear factor 4-alpha (HNF4-alpha)
	NM008281	
	M31042	Immediate early response protein 2 (IER2); T-lymphocyte activated protein; cycloheximide-induced Protein 1 (CHX1)
	U43900	STAM; signal transducing adaptor molecule
	M13177	Transforming growth factor β 1 (TGF-β 1; TGFB1)
	M30644	Fibroblast growth factor 2 (FGF2)
	NM008006	
	M76601	Cardiac myosin heavy subunit alpha isoform (MYH6; MYHCA)
148	AB009453	Transcription factor 21 (TCF21); basic helix-loop-helix factor COR1; POD1
	S71659	LIM homeobox protein 4 (LHX4); GSH4
	S79041	Genomic screened homeobox protein 2 (GSH2)
	U58533	est2 repressor factor (ERF)
	J03770	Homeobox protein D4 (HOXD4); HOX4.2; HOX5.1
	X59252	Homeobox protein 8 (HOX8)
	J03168	Interferon regulatory factor 2 (IRF2)
	S68108	Brahma-related protein 1 (BRG1); swi/snf-related matrix-associated actin dependent regulator of chromatin subfamily a member 4 (SMARCA4)
	D78382	Transducer of erbB2 (TROB; TOB)
	X59421	Fli-1 ets-related proto-oncogene
	M62860	Myelin protein zero
	D31942	Oncostatin M (OSM)
	M29464	Platelet-derived growth factor A subunit (PDGFA; POGF1)
	M69042	PKC-δ; protein kinase C δ type
	U29539	Retinoic acid-inducible E3 protein; stimulated by retinoic acid 13 (STRA13), hematopoetic-specific Protein E3; orfB
	U26967	Cordon-bleu protein (COBL)
149	L38248	LIM homeobox protein 3 (LHX3; UM3)
	X56230	Octamer-binding transcription factor 1 (OCT1; OTF1); NF-A1; POU domain class 2 transcription factor 1 (POU2F1)
	X13721	Homeobox protein 2.4 (HOX2.4)
	L04662	γ-Aminobutyric acid transporter 4 (GABA-A transporter 4; GABT4)
	U59746	B-cell lymphoma protein W (BCLW); BCL2-like protein 2 (BCL2L2)
	M16819	Lymphotoxin alpha (LTA), tumor necrosis factor β (TNF-β; TNFB)
	U12147	Laminin alpha 2 subunit (LAMA2). dystrophia muscularis protein (DV); merosin heavy chain; laminin M subunit
	U22421	Leptin (LEP); obese factor (OB)
133	D10329	CD7 antigen
	D86603	btb and cnc homolog 1 (BACH1)
	U36384	Dermis expressed 1 protein (DERM01)
	M58633	P58/GTA; galactosy transferase associated protein kinase (cdc2-related protein kinase)
	D83698	Activator of apoptosis harakiri (HRK); neuronal death protein 5 (DP5); BID3
	L08235	Clusterin (CLU); clustrin; apolipoprotein J (APOJ); sulfated glycoprotein 2 (SGP2; mSGP2)
	X07414	DNA excision repair protein ERCC1
134	U61155	LIM homeobox protein 2 (LIM2); LHX5
	U20553	p57kip2; cdk-inhibitor kip2 (cyclin-dependent kinase inhibitor 1 B); member of the p21CP1 Cdk inhibitor family; candidate tumor suppressor gene
	U05671	Adenosine At receptor (ADORA1)
	L37663	Acetylcholine receptor alpha 7 neural
	M97017	Bone morphogenetic protein 8A (BMP8A), ostoogenic protein 2 (OPS)
	AF027503	guanylate kinase membrane-associated inverted protein 1 (GUKMI1; MAGI-1)
	M84817	Retinoid X receptor alpha (RXR-alpha; RXRA)
	J03520	Tissue plasminogen activator (T-plasminogon activator PLAT; TPA)
118	X99063	Zyxin(ZYX)
	X14194	Nidogen (NID); entactin (ENT)
119	Y15001	Iroquois-related homeobox protein 3 (IRX3)
	Z23066	Microphthalmia-associated transcription factor (MITF; MI); microphthaltmia-related protein
	X73360	Transducin-like enhancer of split protein 3 (TLE3; ESG)

(*continued on next page*)

Table 2 (*continued*)

Cluster No.	GenBank ID	Gene description
	U65091	Melanocyte-speoific gene 1 (MSG1); Cbp/p300-interacting transactivator with Glu/Asp-rich carboxy-terminal domain 1 (CITED1)
	X97986	Desmocollin 1A/1B (DSC1)
	U81317	Myelin-associated oligodendrocytic basic protein
	U21050	TNF receptor-associated factor 3 (TRAF3); TRAFAMN; C040 receptor-associated factor 1 (CRAF1)
	D83966	Protein tyrosine phosphatase
	L19622	Tissue inhibitor of metalloproteinase 3 (TIMP3); SUN
	AF021031	DiGeorge syndrome chromosome region 6 protein (DGCR6)

plasticity of BMC. In the *F2* time period, clusters 13, 14, 15, 16, 17, 32, 33, and 51 were dramatically changed. In cluster 13, hepatocyte growth factor (HGF) was discovered. HGF is involved in hepatocyte proliferation [27,28]. HGF might also have an important role in GFP/CCl_4 model. In the *F3* time period, clusters 1, 2, 18, and 137 were focused. NumbL is involved in asymmetric division of nerve precursor cells [29]. The HOXD3 genes encode information important for determining the positional relationships of the antero-posterior axis in embryogenesis [30]. NumbL and HOXD3 might have an important role in regulating the plasticity of BMC. In *F4*, clusters 118, 119, 133, 134, 135, 136, 148, 149, 150, 151, 152, and 153 were found. In this period, genes involved in hepatocyte differentiation and homeostasis, such as GPI and HNF4, were focused [31]. This enzyme is essential for the glycolytic metabolism of hepatocytes. In the GFP/CCl_4 model, the level of albumin in bone marrow-derived hepatocytes increased significantly [12]. The fact that an enzyme such as GPI was induced at this period suggests that, at 4 weeks after BMC transplantation, transplanted BMCs begin to possess some of the metabolic functions of hepatocytes. HNF4-α was also upregulated in *F4* period. HNF4 plays an important role in the metabolic regulation of hepatocytes [32,33]. These results might be related with BMC differentiated into functional hepatocyte at this period in GFP/CCl_4 model. VEGF was also upregulated. VEGF promotes vasculogenesis and liver regeneration [34]. VEGF might also have an important role in accelerating the liver regeneration in GFP/CCl_4 model. Gene involved in inflammation such as TNF-R1 was also pointed out in GFP/CCl_4 model. TNF-alpha related inflammation signal is important in the generation of hepatoblast [17]. These results also showed that TNF-α related signal might be important for plasticity of BMC in GFP/CCl_4 model.

Here, we analyzed the change of molecular signature after BMC transplantation in GFP/CCl_4 model in mRNA level. Still many precise things are unconfirmed, but we think the information is useful to understand the mechanism of the plasticity of BMC in GFP/CCl_4 model. In the future, we are planning to further analyze the mechanisms.

Acknowledgements: We thank Dr. Masaru Okabe (Genome Research Center, Osaka University) for the gift of GFP transgenic mice and Mr. Jun Oba for valuable technical support.

References

[1] Alison, M.R. et al. (2000) Nature 406, 257.
[2] Petersen, B.E. et al. (1999) Science 284, 1168–1170.
[3] Theise, N.D., Nimmakayalu, M., Gardner, R., Illei, P.B., Morgan, G., Teperman, L., Henegariu, O. and Krause, D.S. (2000) Hepatology 32, 11–16.
[4] Terada, N. et al. (2002) Nature 416, 542–545.
[5] Ying, Q.L., Nichols, J., Evans, E.P. and Smith, A.G. (2002) Nature 416, 545–548.
[6] Hakelien, A.M. and Collas, P. (2002) Cloning Stem Cells 4, 379–387.
[7] Krause, D.S., Theise, N.D., Collector, M.I., Henegariu, O., Hwang, S., Gardner, R., Neutzel, S. and Sharkis, S.J. (2001) Cell 105, 369–377.
[8] Ianus, A., Holz, G.G., Theise, N.D. and Hussain, M.A. (2003) J. Clin. Invest. 111, 843–850.
[9] Stamm, C. et al. (2003) Lancet 361, 45–46.
[10] Hamano, K., Li, T.S., Kobayashi, T., Hirata, K., Yano, M., Kohno, M. and Matsuzaki, M. (2002) Ann. Thorac. Surg. 73, 1210–1215.
[11] Terai, S., Yamaoto, N., Omori, K., Sakaida, I. and Okita, K. (2002) J. Gastroenterol. 37, 162–163.
[12] Terai, S. et al. (2003) J. Biochem. (Tokyo) 134, 551–558.
[13] McTaggart, R.A. and Feng, S. (2004) Hepatology 39, 1143–1146.
[14] Okabe, M., Ikawa, M., Kominami, K., Nakanishi, T. and Nishimune, Y. (1997) FEBS Lett. 407, 313–319.
[15] Shinoda, K., Mori, S., Ohtsuki, T. and Osawa, Y. (1992) J. Comp. Neurol. 322, 360–376.
[16] Yamamoto, N. et al. (2004) Biochem. Biophys. Res. Commun. 313, 1110–1118.
[17] Watanabe, T. et al. (2002) Dev. Biol. 250, 332–347.
[18] Sakaida, I., Terai, S., Yamamoto, N., Aoyama, K., Ishikawa, T., Nishina, H. and Okita, K. (2004). Hepatology (in press).
[19] Schena, M., Shalon, D., Davis, R.W. and Brown, P.O. (1995) Science 270, 467–470.
[20] Xiao, L., Wang, K., Teng, Y. and Zhang, J. (2003) FEBS Lett. 538, 117–124.
[21] Quaglino, E. et al. (2004) J. Clin. Invest. 113, 709–717.
[22] Ishigaki, S. et al. (2002) FEBS Lett. 531, 354–358.
[23] Nagata, M. et al. (2003) Int. J. Cancer 106, 683–689.
[24] Fujio, K., Evarts, R.P., Hu, Z., Marsden, E.R. and Thorgeirsson, S.S. (1994) Lab. Invest. 70, 511–516.
[25] Zaret, K.S. (2000) Mech. Dev. 92, 83–88.
[26] Heissig, B. et al. (2002) Cell 109, 625–637.
[27] Nakamura, T., Nishizawa, T., Hagiya, M., Seki, T., Shimonishi, M., Sugimura, A., Tashiro, K. and Shimizu, S. (1989) Nature 342, 440–443.
[28] Miyazawa, K. et al. (1989) Biochem. Biophys. Res. Commun. 163, 967–973.
[29] Zhong, W., Feder, J.N., Jiang, M.M., Jan, L.Y. and Jan, Y.N. (1996) Neuron 17, 43–53.
[30] McGinnis, W. (1994) Genetics 137, 607–611.
[31] Massillon, D., Arinze, I.J., Xu, C. and Bone, F. (2003) J. Biol. Chem. 278, 40694–40701.
[32] Li, J., Ning, G. and Duncan, S.A. (2000) Genes Dev. 14, 464–474.
[33] Kamiya, A., Inoue, Y. and Gonzalez, F.J. (2003) Hepatology 37, 1375–1384.
[34] Redaelli, C.A., Semela, D., Carrick, F.E., Ledermann, M., Candinas, D., Sauter, B. and Dufour, J.F. (2004) J. Hepatol. 40, 305–312.

肝臓　45巻9号　505-506（2004）　

＜短　報＞

肝細胞癌に対する新しいバルーンマイクロカテーテルを用いたリピオドール併用肝動脈バルーン閉塞下ラジオ波凝固療法

山崎　隆弘[1)]　木村　輝昭[2)]　浦田　洋平[1)]　丸本　芳雄[1)]　青山　浩司[1)]　石川　剛[1)]
田島　邦彦[1)]　横山雄一郎[1)]　大森　薫[1)]　川口浩太郎[1)]　高見　太郎[1)]　土屋　昌子[1)]
山口　裕樹[1)]　寺井　崇二[1)]　黒川　典枝[1)]　坂井田　功[1)]　沖田　極[1)]

緒言：肝細胞癌に対して経皮的ラジオ波凝固療法(以下RFA)が導入されて，約5年が経過している．その間にも腫瘍の凝固範囲を拡大させる工夫がさまざま報告されており[1～3]，われわれも肝動脈を遮断することで血流によるラジエーター効果を低下させ，凝固範囲を拡大させる肝動脈バルーン閉塞下ラジオ波凝固療法(balloon-occluded RFA：BoRFA)を開発し，有用性について報告した[4,5]．しかし，血管歩行等により，すべての症例で固有肝動脈に通常のバルーンカテーテルを留置するのは不可能であり，そのような症例に対してわれわれはバルーンマイクロカテーテルを用いた肝動脈バルーン閉塞下ラジオ波凝固療法(balloon-microcatheter-occluded RFA；BMoRFA)を開発した[6]．その際用いたバルーンマイクロカテーテルは，Commodore ^{TM} temporary occlusion balloon catheter (Cordis, Johnson and Johnson Co., USA)であったが，5 Fr カテーテルへの挿入が不可能であり，5.1 Fr カテーテルへの交換が必要で手技が煩雑な点，およびその後の検討で予想以上の凝固範囲拡大が得られなかった点[7]が，問題点であり，改良の余地が必要であった．今回，上記の問題点を解決するべく，新しいバルーンマイクロカテーテルを用い，同療法にリピオドールを併用したリピオドール併用肝動脈バルーン閉塞下ラジオ波凝固療法を考案したので報告する．

対象と方法：各種画像診断にて肝細胞癌と診断した4例(4結節)を対象とした．3例が女性，平均年齢69歳，腫瘍径31.3±11.9 mm(24－49 mm)，全例Child-Pugh Aであった．使用装置は，Radionics社のCool-tip RF Systemで，全例3.0 cm針を使用し，1回穿刺で12分間を基本凝固時間としたが，1例のみ腫瘍径が大きいため，引き抜いて12分間追加凝固を行った．使用したバルーンマイクロカテーテルは，Equinox ^{TM} occlusion balloon catheter(Micro Therapeutics, Inc. USA)の4×15 mmのバルーン径を用いた．今回の治療としては，既報[1～6]と異なりリピオドール併用で行った．方法としては，通常の腹部血管造影の手技にて，5 Fr カテーテル(セレコンカテーテル：クリニカルサプライ)を用い，精査を行い，マイクロカテーテルにてTranscatheter arterial chemoembolization(TACE：epirubicin hydrochloride, Mitomycin C, lipiodol使用)を施行し，腫瘍内にlipiodolをpoolingさせた後，Equinox ^{TM} occlusion balloon catheterを担癌領域の肝動脈に留置し，バルーン閉塞後にRFAを施行した．同バルーンマイクロカテーテルは5 Fr カテーテルへの挿入が容易であり，バルーンは造影剤入り生理食塩水を0.2 cc注入することで，4×15 mmのバルーン径が得られた．治療効果判定は，1週間後の造影CTにて施行し，凝固範囲を検討した．

結果：表1のごとく，12分間1回での凝固範囲が検討できたのは，症例2(図1)と4であり，それぞれ，50×47 mm，55×44 mmであった(症例3は，肝梗塞合併のため，計測していない)．同治療法1週間後の造影CTでは，全例で治療部位の早期濃染像は見られなかったが，症例4では，脈管近傍のsafety marginが不足していたため，経皮的エタノール注入療法(PEI)を追加した．合併症では，症例1で発熱の遷延，症例3に肝梗塞を認めたが，保存的に改善した．その他は全例に発熱および疼痛を認めたが，対処療法で改善している．また，一時的に肝機能悪化は認めたが，約1週間後にはほぼ前値に復している．

考察：今回のRFAの工夫としては，新しいバルーンマイクロカテーテルを用いた点およびリピオドール併用肝動脈バルーン閉塞下ラジオ波凝固療法を考案した点の2つである．使用した新しいバルーンマイクロカテーテルは，以前使用したCommodore ^{TM} temporary occlusion balloon catheterとは違い，5 Fr カテーテルでの挿入が可能であり，手技の煩雑さが緩和された．今回の治療法は，肝動脈バルーン閉塞下ラジオ波凝固療法の変法として，ラジエーター効果をより低下させる目的で，リピオドールを併用した．リピオドールは腫瘍内だけでなく，門脈枝にも流入し，腫瘍周囲の門脈血流を低下させること[8]から，動脈および門脈血流の同時遮断効果[9]を狙い，同療法を考案した．通常のバルーンカテーテル(バルーン径9 mm)での検討では，リピオドール併用肝動脈バルーン閉塞下ラジオ波凝固療法において非併用群と比較して，長径では有意差はないものの，短径で有意差を認めている(データ未発表)．リピオドール併用ラジオ波凝固療法での成績は，われわれは持ち合わせていないが，以前の報告[10]よりも凝固範囲は広く，肝動脈閉塞を併用する意義は十分あるものと考える．以前のCommodoreを用いたBMoRFAの1回凝固(12分間)の成績では長径38.3±5.7 mm，短径31.5±4.6 mmと，通常のRFAでの凝固範囲(長径35.3±4.7 mm 短径25.9±3.7 mm)と比較して，短径のみの有意差であった[7]．今回は1回凝固範囲の成績が2例のみであり，なおかつリピオドール併用であるが，50×47 mm，55×44 mmと十分な凝固範囲を認めている．また以前のバルーン径は4×10 mmであったが，新しいバルーンマイクロカテーテルは4×15 mmと短径は4 mmのままであるが，長径が15 mmと長くなっていることが，血流遮断に寄与し，凝固範囲の拡大につながったのかもしれない．今後症例を重ねた検討が必要であるが，新しいバルーンマイクロカテーテルは，通常のBoRFA不可能例の適応に応用可能と考える．また，リピオドール併用肝動脈バルーン閉塞下ラ

[1)]山口大学消化器病態内科学，[2)]同　漢方医学
＜受付日2004年4月13日＞

表1　症例の内訳と成績

症例	性別	年齢	腫瘍径 (mm)	部位	凝固時間 (分)	TACE[a)]の量	凝固径 直径×短径×高さ(mm)
1	女性	70	49	S4	24	EPI[b)]30 mg, MMC[c)]6 mg, lipiodol 6.5 ml	70×53×50
2	男性	67	27	S5	12	EPI[b)]20 mg, MMC[c)]4 mg, lipiodol 3 ml	50×47×55
3	女性	69	25	S8	12	EPI[b)]20 mg, MMC[c)]4 mg, lipiodol 2 ml	−
4	女性	70	24	S5	12	EPI[b)]20 mg, MMC[c)]4 mg, lipiodol 2.5 ml	55×44×55

a) TACE：transcatheter arterial chemoembolization, b) EPI：epirubicin hydrochloride, c) MMC：mitomycin C

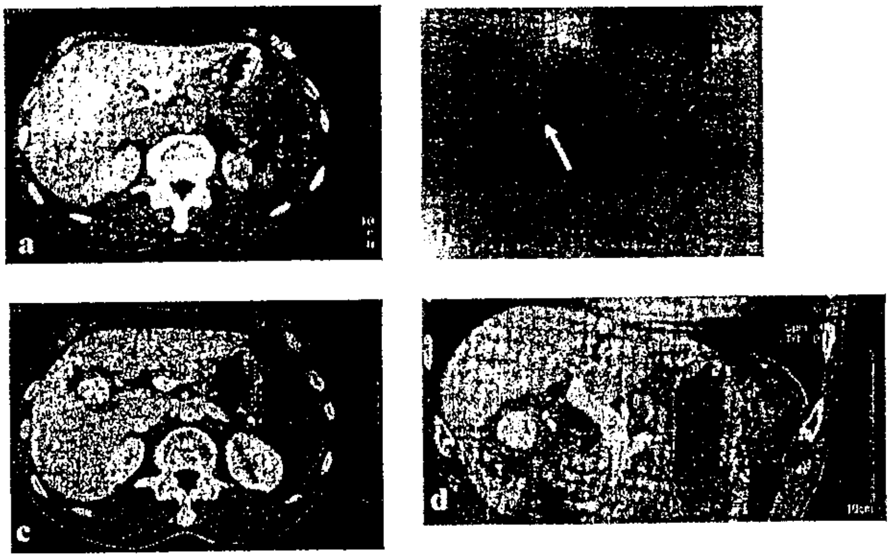

図1　症例2：a：治療前CTA，b：右肝動脈にバルーンマイクロカテーテルを挿入した所(矢印)，c(axial像)，d(sagittal像)：治療後のdynamic CT 50×47×55 mmの凝固範囲を認める

ジオ波凝固療法は，バルーンマイクロカテーテルでの手技でも有効性が示唆された．なお，同治療法は，血管造影検査を行う侵襲性および高価なバルーンマイクロカテーテルを用いる経済面ではデメリットではあるが，最近報告されている5 cm展開針RITA Model 90の単独治療の1回凝固と比較し，凝固範囲が同等以上である点[11]および短期間での精査と治療が可能となる点では十分なメリットがあり，今後はとくに大型肝癌に適応拡大可能と考える．

文献：1) Rossi S, Garbagnati F, Lencioni R, et al：Radiology 217：119−126, 2000　2) 三輪一彦，堀部俊哉，鈴木史郎，他：肝臓 43：172, 2002　3) Kurokohchi K, Watanabe S, Masaki T, et al：Int J Oncol 21, 841−846, 2002　4) 山崎隆弘，黒川典枝，白橋 斉，他：肝臓 41：425, 2000　5) Yamasaki T, Kurokawa F, Shirahashi H, et al：Cancer 95：2353−2360, 2002　6) 山崎隆弘，黒川典枝，高見太郎，他：肝臓 42：688−689, 2001　7) Yamasaki T, Kimura T, Kurokawa F, et al：in submitted　8) Nakamura H, Hashimoto T, Oi H, et al：Radiology 167：415−417, 1988　9) 堀田彰一，中村英明，藤田朋紀，他：肝臓 41：580−581, 2000　10) Kitamoto M, Imagawa M, Yamada H, et al：AJR 181, 997−1003, 2003　11) 三輪一彦，堀部俊哉，小熊一豪，他：肝臓 45：125−126, 2004

自己骨髄細胞を用いた肝硬変症に対する肝臓再生療法

寺井崇二　大森　薫　石川　剛
青山浩司　高見太郎　横山雄一郎
田島邦彦　坂井田功　沖田　極

肝不全患者に対し生体肝移植が行われているが，ドナーの問題，外科侵襲の多さという問題点があり，次世代の肝臓再生療法の開発が求められている。われわれは骨髄細胞（肝幹細胞）の移植療法の有効性を評価するため，GFP/CCl_4モデルを開発し解析してきた。さらに基盤研究を基に臨床研究（自己骨髄細胞を用いた肝臓再生療法）へと展開した。われわれは，肝移植が受けられない肝不全患者に対する新たな治療方法の開発を慎重に進めている。

は じ め に

骨髄中の幹細胞の存在が報告されて以来，再生医療の新たな細胞源として骨髄細胞が注目されている。われわれは『自己骨髄細胞を用いた肝臓再生療法』の臨床開発を進めるため，5 年前より基礎研究を行い，実際に肝硬変症に対する骨髄移植の有効性の検討を骨髄細胞からの肝細胞への分化増殖の *in vivo* 評価モデルを開発し検討してきた[1,2]。このモデルにおいては，持続的な四塩化炭素（CCl_4）投与による肝障害時に骨髄細胞から肝細胞への分化・増殖が確認され，骨髄細胞投与後，肝臓内に投与された骨髄細胞は肝細胞索構造を構築した。発生段階の肝芽細胞の増殖に SEK1，MKK7→SAPK/JNK→c-Jun シグナル系が肝芽細胞の自己複製と生存維持に必須の役割を果たしていることと[3]，持続炎症時に骨髄細胞のアルブミン陽性肝細胞への分化が確認できたことは相似点があると考えられた。さらにわれわれのモデルでは，骨髄細胞投与により，血清アルブミン値の回復や生存率も骨髄細胞の非投与群に比べ有意に改善していた。また肝線維化も有意に改善していた[4]。これらの結果から，自己骨髄細胞を用いた肝臓再生療法は臨床応用可能な次世代の移植医療になりうると考えられた。一方で過去にすでに，循環器領域の虚血性疾患に対しても自己骨髄細胞の注入療法が行われており[5,6]，また骨髄移植そのものについてはすでに 20 年以上の実績がある。われわれは基礎研究の結果を基盤とし平成 13（2001）年 12 月に，『自己骨髄細胞を用いた肝臓再生療法』の臨床研究について，山口大学医学部生命倫理委員会に申請し，安全性・有用性の臨床研究の認可を受けた。さらに約 2 年の期間をかけ，実際に臨床研究を行うための細胞療法部関連の設備，器具を整え，臨床研究の準備を行い，平成 15 年 11 月 14 日に 69 歳男性に対して国内最初の「自己骨髄細胞を用いた肝臓再生療法」の phase I 研究を開始した。本稿ではこの第 1 症例の経過について提示する。

臨床研究の対象症例

今回の臨床研究における対象患者（非代償性肝硬変症）は以下のとおりとした。

T. B. は 3 mg/dL 以下，血小板は 5 万以上，肝細胞癌についてはコントロールできている症例。食道，胃静脈瘤のコントロールが良好であり，また骨髄採取に伴い全身麻酔をかけるので心肺機能は良好の患者とした。

てらい しゅうじ，おおもり かおる，いしかわ たけし，あおやま こうじ，たかみ たろう，よこやま ゆういちろう，たじま くにひこ，さかいだ いさお，おきた きわむ：山口大学医学部先端分子応用医科学講座（消化器病態内科学）

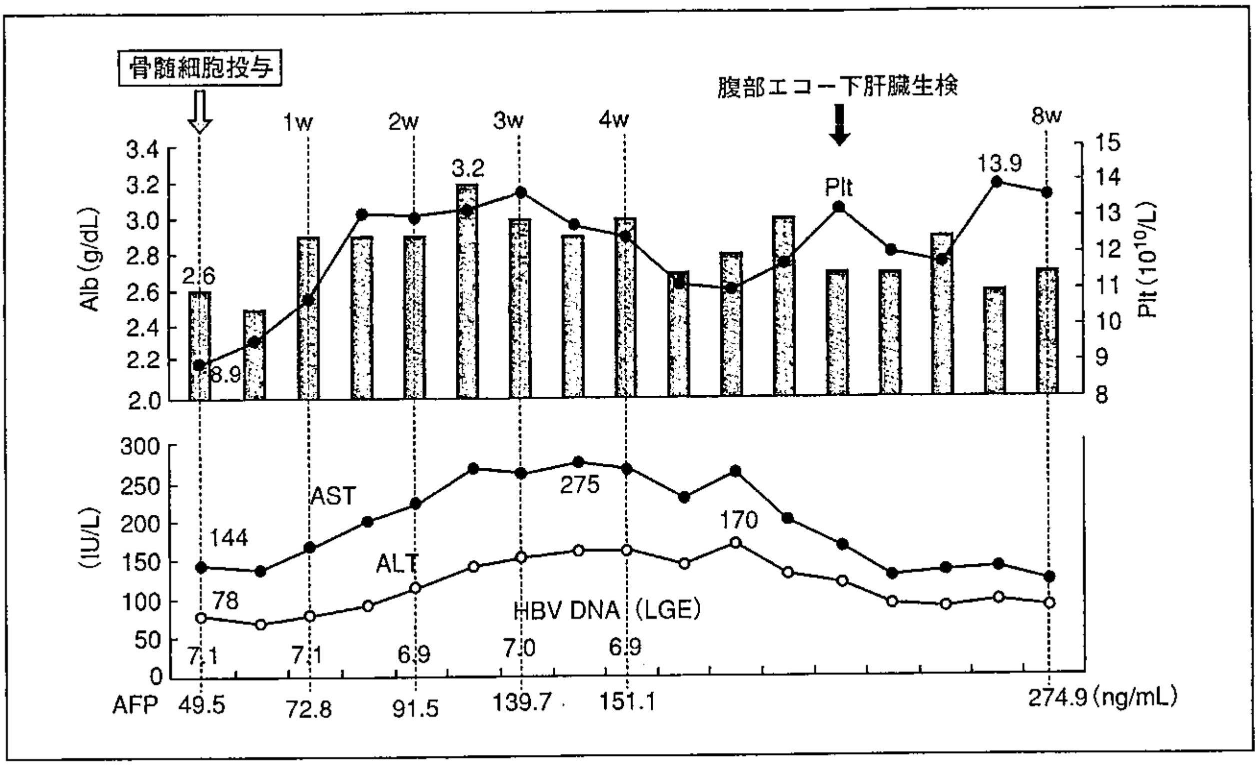

図 1　症例の臨床経過

症例：臨床経過

HBV 陽性非代償性肝硬変症の 69 歳男性に対し，全身麻酔下にて自己骨髄細胞を 400 mL 採取，洗浄後有核細胞の 4×10^9個を採取した。採取した自己骨髄細胞を約 1 時間かけ末梢静脈から投与し，肝臓の再生の誘導の有無について評価した。術中特に大きな合併症もなく，術後血液検査にて骨髄細胞の肝再生に与える影響について評価した。その結果，基礎研究の結果より予測されたように，骨髄細胞投与後より血清アルブミン値は，術前 2.5 g/dL であったものが最大 3.2 g/dL まで改善，また腹部エコーにて腹水の減少を確認し利尿薬の投与量の減量に成功した。また図 1 に経過を示すように AFP（α-フェトプロテイン）も骨髄細胞投与により増加した(図 1)。その他，血小板の値も改善した。また骨髄細胞投与後に施行した肝生検において，hepatocyte nuclear factor-4（HNF4），AFP などの誘導も確認され，肝再生が誘導された可能性が考えられた。

考　　察

症例については術後の経過もよく，骨髄細胞の投与により肝臓再生が誘導された可能性が示唆された。現時点においては，われわれの臨床研究は安全性評価の phase I 研究であり，現在までの 6 例の検討では重篤な副作用の発生はない。今後は慎重に症例を重ね phase I 臨床研究を進めていき，肝臓領域における新たな再生療法としての『自己骨髄細胞を用いた肝臓再生療法』の開発の可能性を評価していきたい。

謝辞　本研究は，厚生労働省厚生科学研究費（基礎研究成果の臨床応用推進事業）の補助を得て推進されている。

文献

1) Terai S, Sakaida I, Yamamoto N, Omori K, Watanabe T, Ohata S, et al. J Biochem 2003；134：551-8.
2) McTaggart RA, Feng S. Hepatology 2004；39：1143-6.
3) Watanabe T, Nakagawa K, Ohata S, Kitagawa D, Nishitai G, Seo J, et al. Dev Biol 2002；250：332-47.
4) Sakaida I, Terai S, Yamamoto N, Aoyama K, Ishikawa T, Nishina H, et al. Hepatology 2004；in press.
5) Hamano K, Li TS, Kobayashi T, Kobayashi S, Matsuzaki M, Esato K. Cell Transplant 2000；9：439-43.
6) Stamm C, Westphal B, Kleine HD, Petzsch M, Kittner C, Klinge H, et al. Lancet 2003；361：45-6.

骨髄細胞から肝細胞への分化転換の制御機構の解析とその臨床応用 ー自己骨髄細胞を用いた肝臓再生療法の基礎的検討ー

寺井崇二*　石川　剛*　大森　薫*　青山浩司*
坂井田功*　沖田　極*

われわれは「自己骨髄細胞を用いた肝臓再生療法」の開発のため，骨髄細胞の肝細胞への分化評価モデル“GFP/CCl 4 モデル”を開発した．このモデルにおいては持続肝障害が続く肝硬変症において骨髄細胞は肝臓へ定着し肝細胞への分化転換していく．一方，肝発生過程において炎症性シグナルは肝芽細胞の発生，増殖は必須であり，肝発生と再生には共通のメカニズムが存在する．さらに，骨髄中の肝幹細胞群の同定のため新規モノクローナル抗体 Liv 8 抗体を用いて基礎的検討をおこなった．これらの結果は自己骨髄細胞を用いた肝臓再生療法は次世代の治療法になり得る可能性を示したのでここに紹介する．

はじめに

B 型，C 型肝炎ウイルスによる肝疾患はいまだ増加傾向を示し，肝細胞癌による死亡は年間の癌死の第 3 位を占めるようになってきた．われわれは臨床の現場において，肝癌治療をおこなっているが，その背景には肝硬変症が合併している患者も多く，肝癌治療そのものの治療法の開発とともに，いかに肝不全を制御するかが重要な問題になる．わが国において生体肝移植が導入されたが，ドナーの不足，外科手術による侵襲の危険性，経済的な問題などからなかなか普及しにくい状況である．これらをふまえて考えた場合，次世代の治療法として肝臓再生療法の開発は重要と考えられる．われわれは，新たに肝不全に対する治療として「自己骨髄細胞を用いた肝臓再生療法」の開発をめざし研究を進めてきたのでここに紹介したい．

［キーワード］
骨髄細胞
肝幹細胞
肝再生
細胞療法
Oval 細胞
Niche
分化転換
肝芽細胞

1．骨髄細胞の肝細胞への分化の可塑性の発見

肝臓は代謝，蛋白合成，解毒などを司る多機能な臓器である．肝臓の発生過程に関してその分化系譜はまだ詳細には明らかにされていないが，われわれは図 1 のように胎児期にまず肝芽細胞が発

*Shuji TERAI, Tsuyoshi ISHIKAWA, Kaoru OMORI, Koji AOYAMA, Isao SAKAIDA, Kiwamu OKITA/山口大学医学部先端分子応用医科学講座（消化器病態内科学）

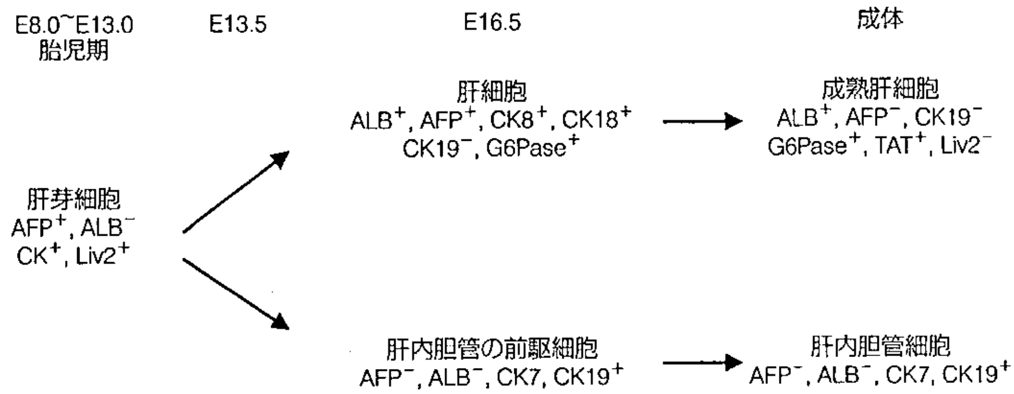

図 1. マウス肝発生過程における分化系譜
E 12.5 における肝臓は肝芽細胞が全体の 2 割，血球系の細胞が 8 割を占める．

生し，その後肝細胞，肝内胆管の前駆細胞に分かれて，成熟肝細胞，肝内胆管細胞が発生すると考えている．また，臓器としての特徴としては胎児期の肝臓は造血臓器としてはたらいていることが特徴である．一方，肝臓に存在する幹細胞そのものについては以前より研究がおこなわれきている．そのなかでも，重篤な肝障害に伴い発生する卵円形をした oval 細胞は肝幹細胞の一つと考えられてきた[1]．この oval 細胞については肝細胞以外に，膵臓，胆管，小腸細胞に分化する可能性が知られている．また，その他方法で，肝幹細胞の同定が試みられ，ラットより小型肝細胞 (small hepatocyte)[2]，Long-Evans Cinnamon (LEC) ラットより肝幹細胞様細胞[3]，胎児肝からは H-CFU-C などが発見されている[4]．これらの細胞の臨床応用については今後，病態に伴うこれらの個々の細胞についての発生制御機構，また局在の変化などについて検討していく必要がある．

一方，骨髄細胞の肝細胞への分化の可塑性については，女性レシピエントに男性ドナーからの骨髄移植後の剖検例において，骨髄細胞が肝細胞に分化することが報告された[5]．これは Y 染色体陽性細胞の存在の有無を肝，胆管細胞にて検討したものであり，骨髄細胞はヒトにおいて肝細胞に分化する可塑性を証明した報告である．このヒトにおける発見は非常に重要で，何らかの機序により骨髄細胞は肝細胞へと分化する可能性があることを示すとともに，肝幹細胞が骨髄中に存在することが明らかになった．また，骨髄細胞の腸管への分化転換についても報告され，骨髄中にはほかの臓器に分化転換する細胞群が存在することが明らかになった[6]．

2．さまざまな肝再生ー部分肝切除による肝再生と oval 細胞の発生を経た肝再生の違いー

ここで一歩はなれて肝再生という現象について考えてみたい．肝臓という臓器は非常に複雑な臓器であり，その構成は，肝細胞，胆管細胞，星細胞，内皮細胞，Pit 細胞，クッパー細胞から成り立ち，肝臓という複雑な代謝系を司っている．肝臓は古来から再生する臓器として知られており，実際に肝切除後には肝再生が起こる．図 2 に示すようにラットの部分肝切除により肝小葉内に存在する肝細胞が肝細胞増殖因子 (hepatocyte growth factor：HGF) などの増殖因子の誘導により増殖し肝再生が起こると考えられている[7](図 2)．一方で oval 細胞の肝細胞化のモデルとしてはアセトアミノフルレン，部分肝切除 (AAF/PH モデル) があるが，このモデルはアセトアミノフルレンの投与により肝細胞の増殖が起こらないようにした状態で肝切除をおこなうモデルであり，この場合